AN ABSTRACT OF THE THESIS OF

PATRICK C. GALLACHER for the degree of Master of Science

Oceanography, (Physical Oceanography) presented on March 15, 1978.

Title: A Description of the Oceanic Mixed Layer at Ocean Station P during August and September 1958 to 1967.

Abstract approved: Redacted for privacy

PEARN P. NIILER

Standard meteorological observations and BT cases taken at Ocean Station P (50N, 145W) for August and September 1958-1967 were used to describe the oceanic mixed layer during the transition from the summer mixed layer regime to the winter mixed layer regime. Synoptic, seasonal and interannual variations are discussed. The mixed layer is wind forced on both seasonal and synoptic time scales. The changes in the heat content of the mixed layer during synoptic deepening events are decoupled from the surface heat flux. The gradual warming trend and periods of layer retreat reflect the surface heating conditions.

Two distinct regimes are found to govern the mixed layer deepening. In the first regime the mixed layer deepens rapidly to a depth comparable to the Thompson depth, in the second the mixed layer erodes the thermocline slowly to a depth scaled by the Monin-Obukhov length.

A Description of the Oceanic Mixed Layer at Ocean Station P during August and September 1958 to 1967

by

Patrick C. Gallacher

A THESIS

submitted to

Oregon State University

in partial fulfillment of
the requirements for the
degree of

Master of Science

Completed March 15, 1978

Commencement June 1978

APPROVED:

Redacted for privacy

Professor of Oceanography

Redacted for privacy

Dean School of Oceanography

Redacted for privacy

Dean of Graduate School

Date thesis is presented March 15, 1978

Typed by Marion Marks for Patrick C. Gallacher

Acknowledgements

I would first like to thank my wife for her patience and encouragement throughout this project. I wish to thank Dr. Niiler for his support, help and advice; also Drs. Paulson, de Szoeke and Garwood for discussions which clarified many difficult points. I wish to thank Mrs. Marion Marks for typing this thesis, Ron Hill for the drafting and Dave Reinert for the photo reduction of the plots; all of which was accomplished under difficult time constraints. This project was supported by the Office of Naval Research under contract #302623112 and the computer work was accomplished at and partially supported by the Milne Computer Center at Oregon State University. The data sets for this project were suppled by Dr. Elsberry of the Naval Postgraduate School, Monterey, California and Dr. Pond of the Institute of Oceanography, University of British Columbia, Vancouver, B.C.

Table of Contents

I. Introduction 1
Statement of the Problem 1
Description of Data 2

II. Discussion of Bimonthly Plots 4
Definition of Variables 4
Discussion of Response 7

III. Discussion of Events 9
Criteria for Events 9
Discussion of Parameters 10
Discussion of Typical Events 14

IV. Summary and Conclusions 16

List of Figures

Figure	
1	The sensible heat flux (light line), long wave radiation (heavy line), solar radiation (open circle), latent heat flux (closed box), total heat flux, air temperature, sea surface temperature, smoothed mixed layer depth, u_*^3, and wind stress for August and September 1958
2	Same as figure 1 for 1959
3	Same as figure 1 for 1960
4	Same as figure 1 for 1961
5	Same as figure 1 for 1962
6	Same as figure 1 for 1963
7	Same as figure 1 for 1964
8	Same as figure 1 for 1965
9	Same as figure 1 for 1966
10	Same as figure 1 for 1967
11	BT casts and anomaly profiles for event 1, 27 Aug 58 0200 GMT - 3 Sept 58 1700 GMT
12	BT casts and anomaly profiles for event 6, 3 Aug 65 0900 GMT - 12 Aug 65 0900 GMT
13	BT casts and anomaly profiles for event 9, 20 Aug 66 0900 GMT - 26 Aug 66 0900 GMT
14	Mixed layer depth (closed circles), Thompson depth (open boxes) and Monin-Obukhov length (closed boxes) for event 1
15	Same as figure 14 for event 6
16	Same as figure 14 for event 9

A Description of the Oceanic Mixed Layer at Ocean Station P during August and September 1958-1967

Introduction

The ocean and atmosphere form a coupled dynamic system with interactions which take place on several time and space scales. The oceanic mixed layer or ocean planetary boundary layer, coupling the atmosphere to the deep ocean, largely determines the rates and scales of the interactions. Thus an understanding of the mixed layer is crucial to resolving large scale problems such as atmospheric forcing of the ocean circulation.

In the last 10 years considerable effort has gone into modeling the oceanic mixed layer. The various models have made significant progress in explaining the physical mechanisms and time scales involved in the dynamics of the mixed layer (see Niiler, 1975 and de Szoeke and Rhines, 1976). A typical method of applying one of these models is to start the model with either actual or simplified atmospheric forcing functions and ocean temperature profiles; the model is then run for some time interval and compared to the ocean thermal structure representative of the time at which the model was stopped. A similar method is to compare the model results with available observations of the ocean structure as a function of time. The adjustable parameters of the model, which are required for a parameterization of the turbulent fluxes, are chosen to "tune" the model to give the best representation of the oceanic structure. The final values of these parameters and their relation to the model equations are indicative of the relative importance of the various possible physical mechanisms and scales in the mixed layer. This type of analysis has yielded considerable insight into the physical behavior of the mixed layer (see Niiler, 1975 and Niiler and Kraus, 1977).

The data analysis in this paper is guided by some simple theoretical considerations. Using standard meteorological and bathythermal (BT) data, the behavior of the mixed layer is described in terms of the wind stress, the surface heat flux, the Thompson depth (Pollard, Rhines and Thompson, 1973) and the Monin-Obukhov length (Garwood, 1977, and Kim, 1976). The Thompson depth evolves as a scale for the mixed layer by relating the vertical shear of the mean current on the entrainment rate at the base of the mixed layer. An increase in the wind stress will excite inertial currents in the upper ocean, which will entrain water from below the mixed layer through the shear exerted at the base of the inertial current. This entrainment will continue until the Coriolis force has rotated the current normal to the wind stress. This depth is given by the Thompson depth. The Monin-Obukhov length is the depth at which the turbulent KE input by the wind stress is balanced by the PE increase due to surface heating.

The data set for this study consists of standard meteorological observations taken at 3 hourly intervals and BT and XBT casts made at irregular intervals. The meteorological observations included air temperature, sea surface temperature, wet bulb temperature, wind speed, wind direction, sea level atmospheric pressure and total cloud cover. The BT casts ranged in depth from 95 m to 300 m, and were digitized at 5 m intervals. The time interval between casts depended on weather conditions and ranged between 20 minutes and 2 days. The measurements were taken at Ocean Station P (50N, 145W) by two vessels manned by the Marine Services Branch of the Canadian Ministry of Transport. Each ship remained on station for 6 weeks and was then relieved by the alternate ship, thus providing a continuous record of the conditions at Ocean Station P.

From the weather ship data we obtained the air temperature, sea surface temperature, wet bulb temperature, sea level atmospheric pressure, wind speed, wind direction, total cloud cover and BT casts for August and September 1958 to 1967. These variables were then used to produce time series of sensible and latent heat fluxes, solar and long wave radiation (effective back radiation), the oceanic friction velocity cubed, the wind stress and the mixed layer depth for each of the 10 years. Twelve synoptic scale events were selected from the time series during which the BT data showed significant changes in the mixed layer depth; these are marked by |————| in Figs. 1-10. For these events, the vertical temperature structure, the anomaly temperature structure, the Thompson depth, the Monin-Obukhov length, the daily anomalous heat content and the correlation between the daily anomalous heat content and the daily mean surface heat flux were calculated.

The mixed layer deepening is wind forced for all events; rapid deepening occurs when the mixed layer depth is less than the Thompson depth whereas the mixed layer slowly erodes the thermocline when the mixed layer is deeper than the Thompson depth. Periods of mixed layer retreat correspond to shallow values of the Monin-Obukhov length which are the result of decreased wind speeds and increased surface heating. The changes in the heat content of both the mixed layer and the upper 100 m of the water column show no correlation with the surface heat flux during the events.

Discussion of Bimonthly Time Series

Figures 1 through 10 show the time series for the years 1958 to 1967. The air temperature and sea surface temperature (hereafter referred to as SST) were plotted directly from the data. The mixed layer depth was defined as the deepest depth with a temperature less than 0.2°C lower than the temperature at 5 m. That is the mixed layer depth, d_m, is defined such that

$$T(d_m) \geq (T(5) - 0.2) ,$$

and

$$T(d_m + 5) < (T(5) - 0.2) ;$$

where $T(d)$ is the temperature in degrees Centigrade at a depth of d meters below the surface. The bimonthly time series of mixed layer depths were then smoothed with a 24 hour equal weight, running mean filter which effectively removed the diurnal variations. The resultant wind stress, τ , was defined as

$$\tau = \rho_a C_D (U_x + U_y)^2 ,$$

where U_x is the eastern component of the wind (in m/sec) and U_y is the northern component of the wind (in the vector sense of direction), ρ_a is the density of air, and C_D is the drag coefficient. The ocean friction velocity cubed is given by

$$u_*^3 = (\rho_a/\rho_w C_D U^2)^{3/2} ,$$

where ρ_w is the density of sea water. The drag coefficient, used for the plots of τ and u_*^3 was calculated using the empirical formula

derived by Smith and Banke, 1974

$$10^3 C_D = 0.63 + 0.066\ U\ ;$$

however it was later concluded that the accuracy implied by this formula was greater than the accuracy of the data set and the drag coefficient was taken as

$$C_D = 1.5 \times 10^{-3}\ ,$$

for all later calculations. The result of using the Smith and Banke drag coefficient is that the maximum values of τ and u_*^3 shown on the plots will be larger than values commonly used in the literature. The surface heat fluxes were calculated using the following formulae:

$$QS = \rho_a C_p C_T U (T_s - T_a) \qquad \text{(sensible heat flux)},$$

$$QH = \ell_v C_q U (q_s - q_a) \qquad \text{(latent heat flux)},$$

$$QL = \varepsilon\sigma T^4 (0.254-0.00495e)(1-0.9c) \qquad \text{(long wave radiation)},$$

$$QR = (1-0.62c+0.0019\alpha)(199.1-133.4\cos\phi + 75.7\sin\phi + 5.08\cos\phi-2.29\sin 2\phi \qquad \text{(solar radiation)},$$

$$QT = QS + QH + QL - QR \qquad \text{(total heat flux)};$$

where C_p is the specific heat of dry air, C_T is the Stanton number, T_s is the SST, T_a is the air temperature, ℓ_v is the latent heat of vaporization, C_q is the Dalton number, q_s is the absolute humidity at the sea surface (taken as 98% of the absolute humidity at the SST and the saturation vapor pressure), q_a is the absolute humidity at the reference height, ε is the emissivity of the sea surface, σ is the Stefan-Boltzman constant, e is the air pressure, c is the total cloud cover in tenths, α is the solar elevation at local noon and $\phi = (t-21)(360/365)$ where t is the Julian date. Table 1 is a tabulation of the formulae or the numerical values and references for the parameters

defined above. The formulae for QS and QH are taken from Pond, Fissel and Paulson, 1973. The formula for QL is from Reed, 1976 and the formula for QR is from Reed, 1977. The sign convention for the surface heat fluxes is such that a positive heat flux indicates oceanic heating.

In the bimonthly (seasonal) plots u_*^3 is scaled such that the just discernable noise, for example during August 24, 1959, represents a wind speed of approximately 8.5 m/sec which is the average wind speed over the 10 year period. The maximum wind speeds for each year range from 15 m/sec in 1965 to 28 m/sec in 1959. Thus the peaks in u_*^3 represent storms characterized by above average winds. The daily average solar heat flux is shown by the open circle and the daily average latent heat flux by the closed boxes. The lack of either direct solar radiation measurements or observations of cloud type and height preclude the resolution of solar radiation for periods shorter than one day. The 3 hourly, instantaneous sensible heat flux is the heavy line and the 3 hourly, instantaneous long wave heat flux is the light light.

The annual cycle of the mixed layer at OS P has been discussed by Tabata, 1965 and Tully and Giovando, 1963. They postulated that the heating cycle begins in April when the mixed layer begins to retreat as the effect of increasing solar heat flux exceeds the wind mixing. The warming continues through the summer under low wind conditions creating a mixed layer of depth 0 to 10 meters. During August and September increasing numbers of storms begin to mix the upper ocean driving the mixed layer depth to 40 or 50 meters. From October through March the increased storm activity and reduced solar heating combine to mix the upper ocean to the depth of the permanent pycnocline, between 150 to 200 meters. We

will look in detail at the transition period of August and September when the summer regime gives way to the winter regime.

Figures 1-10 show this transition period for 1958 through 1967. The years 1960 through 1964 and 1966, 1967 might be considered normal years. They are all characterized by increasing storm activity and decreasing mixed layer depth (MLD) during the two month period. 1958 and 1959 show early winters with the MLD being deeper than usual and the storm systems well established on the first of August. Conversely 1965 represents a year of very low storm activity, with virtually no downward trend in the MLD, and the strongest positive SST trend. Yet the MLD is rather deep on the first of August (30 m) and there is vigorous mixed layer activity with the MLD cycling over 20 m several times.

The seasonal plots also show several interesting correlations and seasonal trends. In every year the MLD increases through the two month period, although the increase is small in 1965, as discussed above. The SST, which would be expected to follow the MLD trend, increases for 1959, 1964 and 1965, shows a zero trend in 1960, 1961, 1962 and 1963 and has a negative trend only in 1958, 1966 and 1967. It is interesting to note that 1959 had more storms than average but the SST did not decrease. The SST does show a correlation with the MLD on a synoptic scale; for example the deepening event which starts on August 6, 1961 correlates with a decrease in SST which occurs on the same day. The SST does correlate very well with the air temperature throughout the entire period for all years. The average total heat flux is positive for all years and is small in 1967. The total heat flux becomes zero or negative only during

violent storms and it quickly becomes positive after the storms. The solar heat flux dominates the surface heat budget on the seasonal time scale in all cases; only during storms is the solar heat flux balanced or exceeded by the latent heat flux. In all cases the sensible and long wave heat fluxes are an order of magnitude smaller than the solar and latent heat fluxes. Thus they make no significant contribution to the heat budget during this period.

The seasonal plots definitely show August and September to be a transition period between the summer and winter mixed layer regimes. The motion of the MLD is shown to be step-like with the mixed layer deepening during storms and retreating between storms. The downward trend of the MLD shows that the wind generated energy available for mixing exceeds the solar energy available for warming over the two month period. The negative MLD trend and positive or zero SST trend demonstrate that the dynamics of the mixed layer are essentially decoupled from the surface heat flux during this period and the upper ocean continues to increase its heat storage during August and September.

Discussion of Events

From the 10 year, bimonthly data set discussed in the last section 12 mixing events were chosen for further study. The criteria for an event was that there be a marked, rapid deepening of the mixed layer and that the time span of the event contain a sufficidnt number of BT casts to show the behavior of the upper ocean thermal structure. The events, cataloged in Table 2, vary from 6 to 14 days; the time span was selected to allow a series of BT casts before and after the storm since in general, no casts were made during the height of the storms.

For each event the BT casts were plotted with the mixed layer depth and the depth of the bottom of the entrainment zone marked on each cast, and the casts were truncated at 100 meters. The entrainment zone is taken to mean the region of rapid change in temperature with depth found immediately below the mixed layer; i.e. the transient thermocline. The bottom of the entrainment zone, d_e , was defined as the deepest depth having a temperature more than 0.5°C warmer than the temperature 5 meters below it; i.e.

$$T\ (d_e) > (T\ (d_e + 5) + 0.5)\ .$$

Anomaly profiles were defined as the profile of $\Delta T(d)$ where

$$\Delta T(d) = T(d) - T_A(d)$$

and $T_A(d)$ is the temperature at the depth, d, averaged over the event. The anomaly profiles clearly show the heat flux in the water column as the mixed layer advances or retreats. Three regions are delineated by the anomaly profiles corresponding to the region between the surface and the

first zero crossing, from the first to the second zero crossing and from the second zero crossing to 100 meters. These three regions correspond roughly to the mixed layer, the entrainment zone and the deep or advective zone in the BT casts. A shallow, warm cast, compared to the event average, will produce an anomaly profile with a positive temperature anomaly in the upper region, a negative anomaly in the entrainment region, and no anomaly in the deep portion of the profile. Conversely, a deeper, colder than average BT cast will produce an anomaly profile with a negative anomaly in the upper region, a positive anomaly in the entrainment region, and no anomaly in the deep region. Anomalies which occur in the deep zone are assumed to be the result of horizontal advection; however this may not always be the case. The anomaly profiles show the vertical flux of heat associated with the movement of the mixed layer. Periods of mixed layer advance are noted by the pattern of the mid water anomaly in time. The mid water anomaly, which is negative for the shallow starting profiles approaches zero and then changes sign as the layer becomes deeper than average. Periods of mixed layer retreat begin with the formation of a small positive anomaly at the base of the upper zone, a negative anomaly then begins to grow just below the positive anomaly. When the mixed layer has retreated the negative anomaly becomes the entrainment zone anomaly and the positive anomaly is distributed through the mixed layer.

The 12 events show very similar characteristics despite the variations in the initial and final depth of the mixed layer, u_*^3, and the surface heat flux; therefore we will present the results of only 3 events (1, 6 and 9). The BT casts and anomaly profiles for the three events,

Figures 11-13, show typical deepening and retreat periods. The anomaly profiles show a case of mixed layer advance in event 1 at day 2 0600 GMT followed by an occurrence of mixed layer retreat beginning at day 3 0100 GMT. Other examples of mixed layer advance and retreat are shown throughout all three events. The vertical redistribution of heat through the water column can be seen by noting the changes in the sign and depth of the mid water anomaly. For example, the cases mentioned above clearly show a downward heat flux as the mixed layer advances and an upward heat flux accompanying the layer retreat. Event 6 shows the effect of a large remnant mixed layer on the anomaly profile. During days 2 and 3, the BT casts show a shallow mixed layer which has formed, due to surface heating, over a previous, deeper mixed layer. The motions of the MLD shown in the BT casts are not well represented in the anomaly profiles until after day 5 when the new mixed layer has been mixed down through the older mixed layer. Thus the anomaly profiles appear to be most useful during periods of stormy mixed layer activity.

The anomalous heat content can be calculated for the three zones of the anomaly profiles defined by the two zero crossings, the surface and the 100 m depth. For instance the anomalous heat content in the mixed layer region is given by

$$\Delta H = \rho_w \, C_{pw} \int_0^{D_1} \Delta T(z) \, dz \, ,$$

where D_1 is the depth of the first zero crossing and C_{pw} is the specific heat of sea water. The total daily surface heat flux, HT , and the heat content of daily averages of the anomaly profiles for the mixed layer, ΔH_M, entrainment, ΔH_E, and deep zones, ΔH_D, and for the entire water column, ΔH_T , from 0-100 m were computed for each event.

In addition the cross correlations of ΔH_T and HT and ΔH_M and HT were calculated for each event. The results are shown in Table 3 for events 1, 6 and 9.

There is no significant correlation, at the 95% confidence level, between ΔH_T and HT or between ΔH_M and HT for any event demonstrating the independence of the mixed layer dynamics and the thermal forcing on synoptic time scales. In general ΔH_D is roughly an order of magnitude smaller than ΔH_E or ΔH_M for all three events. We would expect that a non zero ΔH_D would imply horizontal advection; however, the largest values of ΔH_D correspond to major mixing events, as indicated by the change in sign of ΔH_M and ΔH_E . Thus it is possible that for deepening events, as shown for day 7 of event 1, the large values of ΔH_d are the result of internal waves generated in the entrainment zone. In the cases of mixed layer retreat, day 7 of event 6 and day 4 of event 9, the large values of ΔH_D are due to the remnant mixed layer. The other cases of large ΔH_D occurring at day 3 in event 6 and at day 5 in event 6, are probably the result of horizontal advection. Since these other occurrences appear in 4 out of the 22 days shown in Table 3, advection does not appear to play an important role in the mixed layer dynamics at Ocean Station P during August and September. The very large values of ΔH_M during days 8 and 9 of event 6 should be noted, as should the depth of the top layer on these days. Neither the total surface heat flux nor the air temperature show a correspondingly large anomalous value; therefore this might be the result of a patch of warm water moving through the area, possibly caused by a southern shift in the path of the Northern Pacific current. The result of such a shift would be to allow the warmer water from the center of the North Pacific gyre to move past Ocean Station

P . This possibility is also supported by the fact that the warm water anomaly extends down to 80 meters.

Niiler, 1975, de Szoeke and Rhines, 1976 and Niiler and Kraus, 1977 have shown that the deepening of the mixed layer is controlled by balances between different terms in the turbulent kinetic energy equation for different time and space scales. This behavior leads to the existence of several distinct mixing regimes each with its own characteristic scales. Two of these regimes have time and space scales which can be resolved with this data set. The first regime, which has a time scale of about 10 hours, is governed by the vertical shear at the base of the wind generated inertial current and the Coriolis force. The depth scale for this regime was derived by Pollard, Rhines and Thompson, 1973, and is given by the Thompson depth,

$$d_T = \frac{2^{3/4} u_*}{(Nf)^{1/2}} ,$$

where N is the Brunt-Väisälä frequency below the mixed layer and f is the inertial frequency. Changes in the wind generate inertial currents in the upper ocean; these result in a sharp vertical gradient in the horizontal velocities at the base of the inertial layer.

Pollard, Rhines and Thompson have argued that the shear stresses, set up by the velocity gradient, feed energy into finite amplitude interfacial waves which break up the interface when the ratio of the hydrostatic stability to the shear stability, i.e., the local Richardson number, falls below some critical value. The breaking of the interfacial waves increases entrainment of fluid from below, which increases the layer depth and the

vertical shear until the Richardson number is again above its critical value. Pollard, et al. equated the local Richardson number with the bulk Richardson number and determined that the critical Richardson number should be O(1). With these assumptions the Thompson depth can be obtained from solving the vertically integrated, time dependent equations for the horizontal momentum. This type of argument, involving a critical value for the stability parameter, implies that a mixed layer with $d < d_T$ initially will deepen rapidly (within f^{-1}) to d_T. The second regime, with a time scale of 10 days, has a depth scale defined by the Monin-Obukhov length,

$$d_M = \frac{2\ u_*^3}{\left(\frac{\alpha g\ QT}{C_{pw}\rho_w}\right)}$$

where α is the thermal coefficient of expansion for sea water and (taken to be 0.0002/°C) and g is the acceleration due to gravity. The Monin-Obukhov length is the ratio of the available mixing energy due to the wind over the convective energy put in by surface heating. So this regime is characterized by a balance of the wind mixing and the surface heating, which implies that the mixed layer will slowly erode the thermocline to a depth of $O(d_M)$. In this context the Monin-Obukhov length is only meaningful during periods of net surface heating. N is given by

$$N = \left(\alpha g \frac{\partial T}{\partial z}\right)^{1/2}$$

and it was computed from the temperature gradient at the mid-point of the entrainment zone. The Thompson depth was calculated for each BT cast

during the events. The Monin-Obukhov length was calculated once a day at local noon using the daily averaged QT and a daily averaged value of u_*^3.

Figures 14-16 show the mixed layer depth, d_T and d_M for events 1, 6 and 9. During event 1 the mixed layer depth is between d_T and d_M for the entire event. This behavior of the mixed layer is attributed to the severity of the storms and the initially deep mixed layer in 1958. The mixed layer deepens 15 m in the first 24 hours of the event then remains relatively constant for the remaining days due to the decrease in u_*^3 as shown by the decrease in d_T. Finally on days 5 and 6 the daily value of u_*^3 has decreased to a point where the heating becomes of the same order of magnitude as the wind stirring, d_M decreases and the mixed layer retreats. Event 6 begins with a shallow mixed layer depth and a shallow d_M both due to low wind speeds. The wind picks up increasing d_M such that d_T is now the dominant depth scale and the mixed layer deepens 10 m in 12 hours between days 2 and 3. The mixed layer then continues to deepen slowly until it stabilizes on day 5. The rising d_M, caused by the reduced u_*^3 and increased heating, pushes the mixed layer depth up until on day 9 the mixed layer depth has retreated to 15 m. In event 9, the pattern of an initially shallow mixed layer with a depth less than d_T which deepens below d_T in roughly 12 hours where it stabilizes until d_M rises again immerges. Despite the small number of BT casts and the requirement that D_M can only be calculated from daily averages the data shows that the mixed layer appears to be one regime when the mixed layer is above d_T and another when it is between d_T and d_M. Thus we can distinguish both the mechanism responsible for forcing the mixed layer, i.e. the wind, and the type of deepening regime on synoptic time scale.

Conclusions

We have shown that the mixed layer in the Northeastern Pacific is wind forced on both seasonal and synoptic time scales during August and September. Additionally the period of August and September represents a transition from the typical summer regime to the typical winter regime during which the mixed layer begins to deepen toward its winter value in spite of solar heating. On a synoptic scale, the mixed layer dynamics are dominated by mechanical mixing with the heat flux in the water column being a function of the mixing.

The Thompson depth and the Monin-Obukhov length can be calculated from available data and yield useful information concerning the mixed layer dynamics. On a synoptic scale, these parameters revealed two separate mixing regimes one being controlled by the balance between u_*^3 and QT, and the other by the strength of the vertical shear and the local Richardson number. These regimes act on different vertical space scales and time scales and noticeably affect the rate of mixed layer advance and retreat. We have also been able to show that horizontal advection is not important during this period, at least not for synoptic scales. We have also shown the possibility of a definite vertical advection during the time of rapid mixed layer advance and retreat. Also the large value of d_M shows that the controlling factor for deepening the mixed layer is the available wind not a balance between the competing driving mechanisms of wind stirring and surface heating.

The net heat flux into the ocean is less during August and September than during the summer months (Tully and Giovando, 1963); however the heat is mixed to significantly greater depths. This increases the

capacity of the upper ocean to store heat by making more water available and increases the potential energy of the water column. This increased potential energy has no local effect; however horizontal variations in the potential energy could give rise to geostrophic currents. The observation that the maximum potential energy lags the maximum surface heat flux was also found by Gill and Turner (1976).

Table 1

Parameter	Formula or Numerical Value	Reference
C_T, Stanton number	1.5×10^{-3}	Pond, Fissel, Paulson (1974)
C_q, Dalton number	1.5×10^{-3}	ibid
C_p, Specific heat of dry air	0.2404 cal $gm^{-1}K^{-1}$(@ 12°C)	Iribarne and Godson (1973)
ℓ_v, Latent heat of vaporization	2.472×10^{6} J kg^{-1}(@ 12°C)	ibid
q_a, abs. humidity at reference height	$\xi \rho_a ep^{-1}$	ibid
q_s, abs. humidity at sea surface	$0.98 \xi \rho_a e_w p^{-1}$	ibid
where: $\xi = R_d/R_v$ 0.622		ibid
ρ_a, density of dry air 1.25×10^{-3} gm cm^{-3}(@ 12°C)		ibid
p, atmospheric pressure		Data
e, vapor pressure $f(T_a, T_w, p)$		List (1971)
e_w, saturation vapor pressure $f(T_s, T_w, p)$		List (1971)
ε, emissivity of sea surface	0.98	Reed (1976)
σ, Stefan-Boltzman constant	0.813×10^{-10} cal $cm^{-2}K^{-4}min^{-1}$	ibid
α, solar elevation	$\sin^{-1}(\sin\delta \sin\Phi - \cos\delta \cos\Phi \cos t_h)$	Paltridge and Platt (1976)
where: δ, solar declination (a function of the julian date)		ibid
t_h, hour angle (= 0 for local noon)		ibid
ϕ, latitude		Data

Table 2

EVENT	START TIME	STOP TIME	NO. OF DAYS
1	27 Aug 58 0200	3 Sept 58 1700	7
2	13 Sept 58 0900	18 Sept 58 0900	5
3	3 Aug 61 0200	17 Aug 61 0900	14
4	20 Aug 61 0900	25 Aug 61 0900	5
5	28 Aug 61 0900	2 Sept 61 1000	5
6	3 Aug 65 0900	12 Aug 65 0900	9
7	18 Aug 65 0900	25 Aug 65 0900	7
8	8 Sept 65 0900	19 Sept 65 0900	11
9	20 Aug 66 0900	26 Aug 66 0900	6
10	13 Sept 66 0900	24 Sept 66 0900	11
11	3 Aug 67 0900	14 Aug 67 0900	11
12	15 Aug 67 0900	27 Aug 67 0900	12

Table 3

Daily surface heating and daily anomalous heat contents. Depths of the top two layers are shown in parenthesis (meters). (Units: 10^6 joules/m^2).

EVENT	DAY	ΔH_M	ΔH_E	ΔH_D	ΔH_T	HT	Co<ΔH_T,HT>	Co<ΔH_M,HT>
1	1	19.7 (25)	-39.7 (45)	.3	- 19.7	5.8	0.03	0.29
	2	21.8 (35)	-21.5 (100)	0.0	0.3	2.9		
	3	- 1.1 (10)	3.7 (35)	- 46.6	- 43.9	4.1		
	4	- 9.2 (30)	2.3 (35)	- 15.6	- 22.5	3.1		
	5	- 15.9 (30)	13.5 (50)	- 0.2	- 2.6	3.6		
	6	- 9.6 (30)	41.8 (70)	- 0.1	32.2	3.4		
	7	- 6.7 (30)	65.8 (100)	0.0	59.1	4.8		
6	1	- 46.4 (35)	0.9 (40)	- 0.5	- 46.0	-1.9	0.03	0.07
	2	- 39.6 (35)	10.9 (65)	- 3.5	- 32.2	0.5		
	3	- 24.5 (30)	15.2 (50)	- 12.2	- 21.4	7.0		
	4	- 9.9 (30)	18.3 (50)	- 0.0	8.3	5.7		
	5	- 8.9 (15)	7.8 (35)	- 27.6	- 28.8	5.2		
	6	- 3.5 (10)	6.7 (30)	- 59.8	- 56.6	6.2		
	7	- 4.1 (10)	3.9 (30)	-109.4	-109.6	2.6		
	8	105.7 (70)	- 7.5 (100)	0.0	98.2	2.3		
	9	159.9 (80)	- 2.9 (100)	0.0	157.0	3.6		
9	1	- 59.9 (55)	9.6 (100)	0.0	- 50.3	6.7	0.62	0.71
	2	- 31.3 (40)	9.6 (100)	0.0	- 21.7	6.1		
	3	- 24.4 (25)	22.6 (50)	- 0.1	- 1.9	3.8		
	4	- 8.1 (25)	30.6 (45)	- 21.9	0.5	3.6		
	5	31.8 (40)	- 0.9 (45)	2.2	33.2	13.0		
	6	42.1 (40)	- 0.3 (45)	1.1	42.9	11.5		

Figure 1

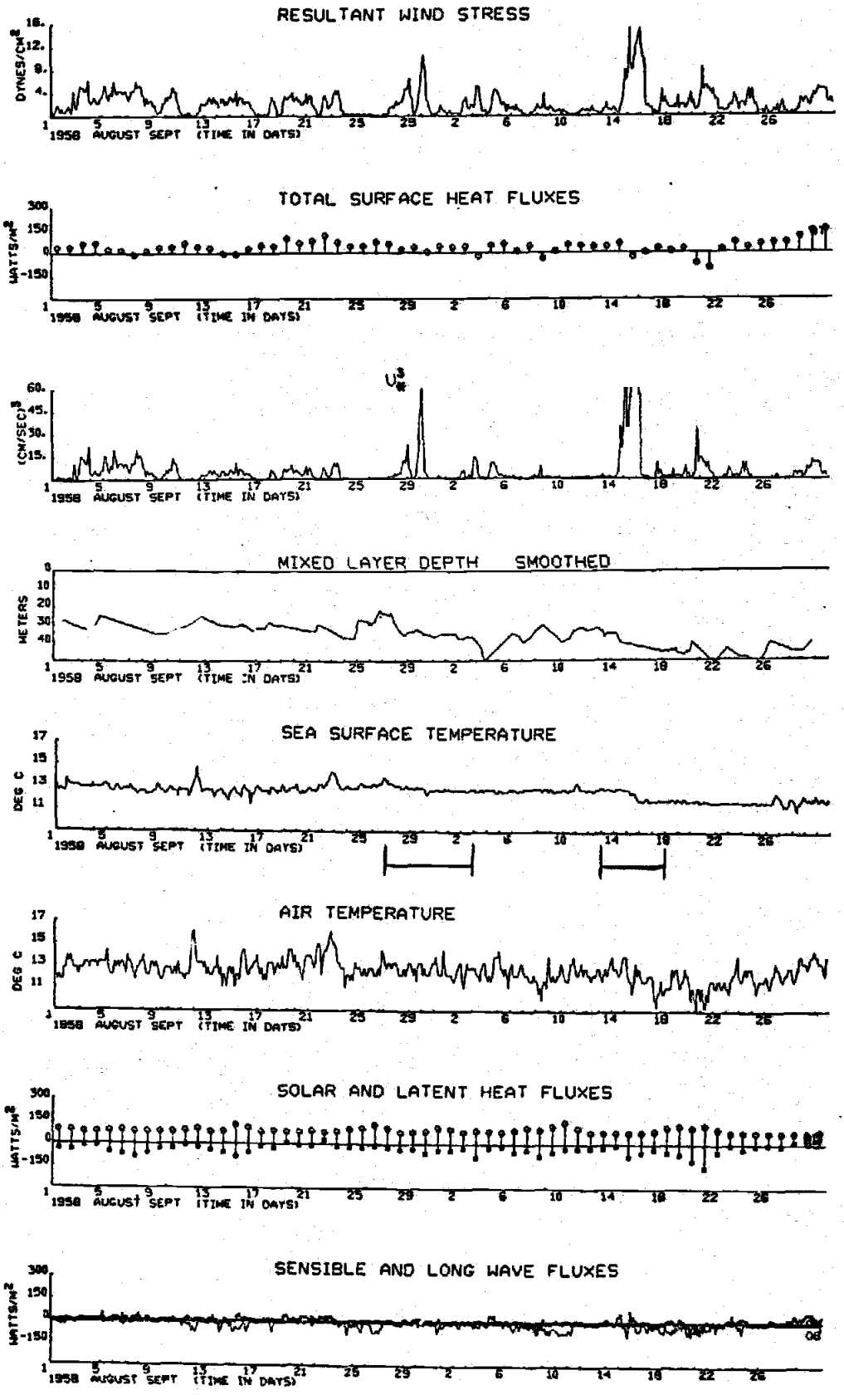
RESULTANT WIND STRESS
DYNES/CM²
TOTAL SURFACE HEAT FLUXES
WATTS/M²
(CM/SEC)³
MIXED LAYER DEPTH SMOOTHED
METERS
SEA SURFACE TEMPERATURE
DEG C
AIR TEMPERATURE
DEG C
SOLAR AND LATENT HEAT FLUXES
WATTS/M²
SENSIBLE AND LONG WAVE FLUXES
WATTS/M²
1958 AUGUST SEPT (TIME IN DAYS)

Figure 2

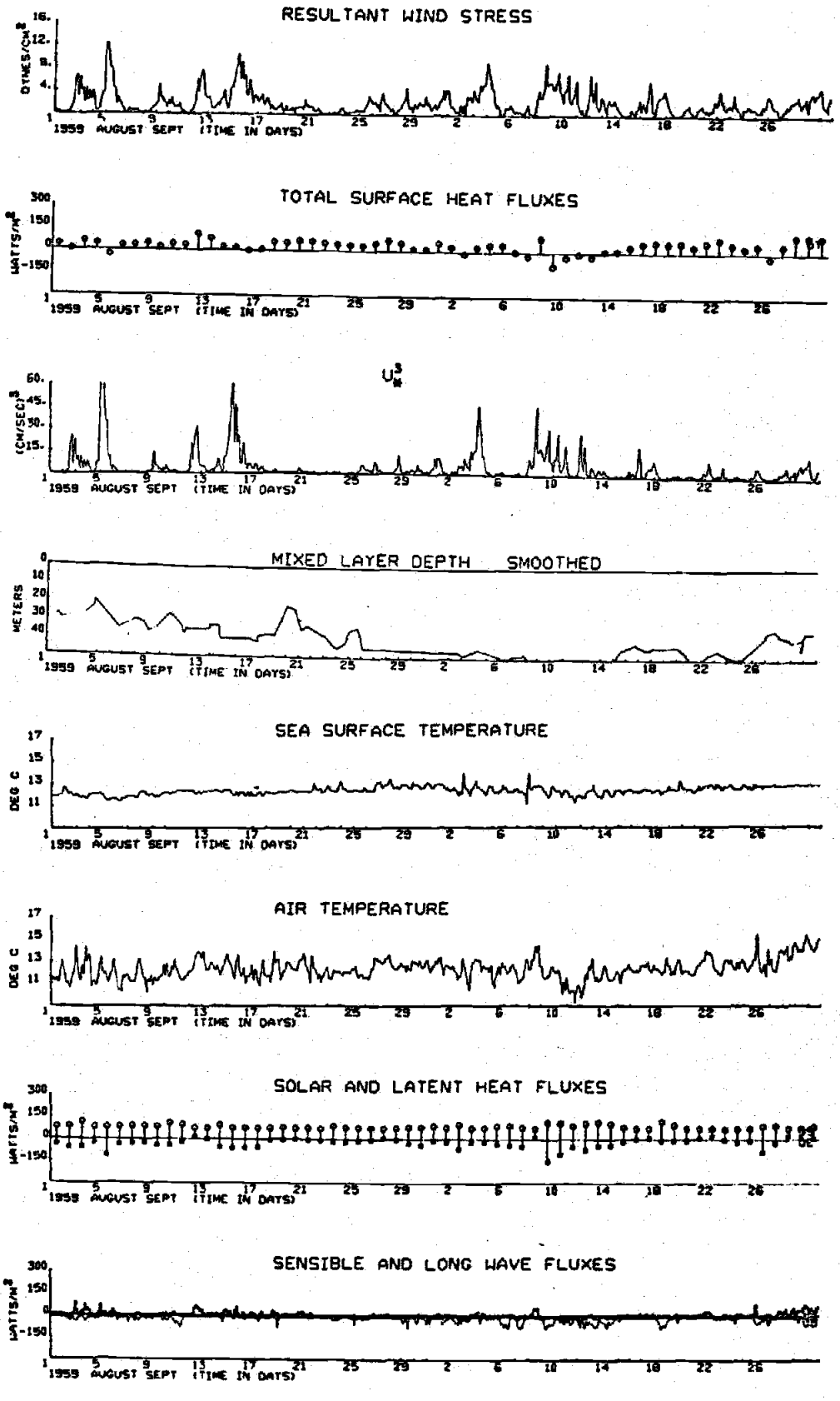
RESULTANT WIND STRESS
DYNES/CM²
TOTAL SURFACE HEAT FLUXES
WATTS/M²
(CM/SEC)³
MIXED LAYER DEPTH SMOOTHED
METERS
SEA SURFACE TEMPERATURE
DEG C
AIR TEMPERATURE
DEG C
SOLAR AND LATENT HEAT FLUXES
WATTS/M²
SENSIBLE AND LONG WAVE FLUXES
WATTS/M²
1959 AUGUST SEPT (TIME IN DAYS)

Figure 3

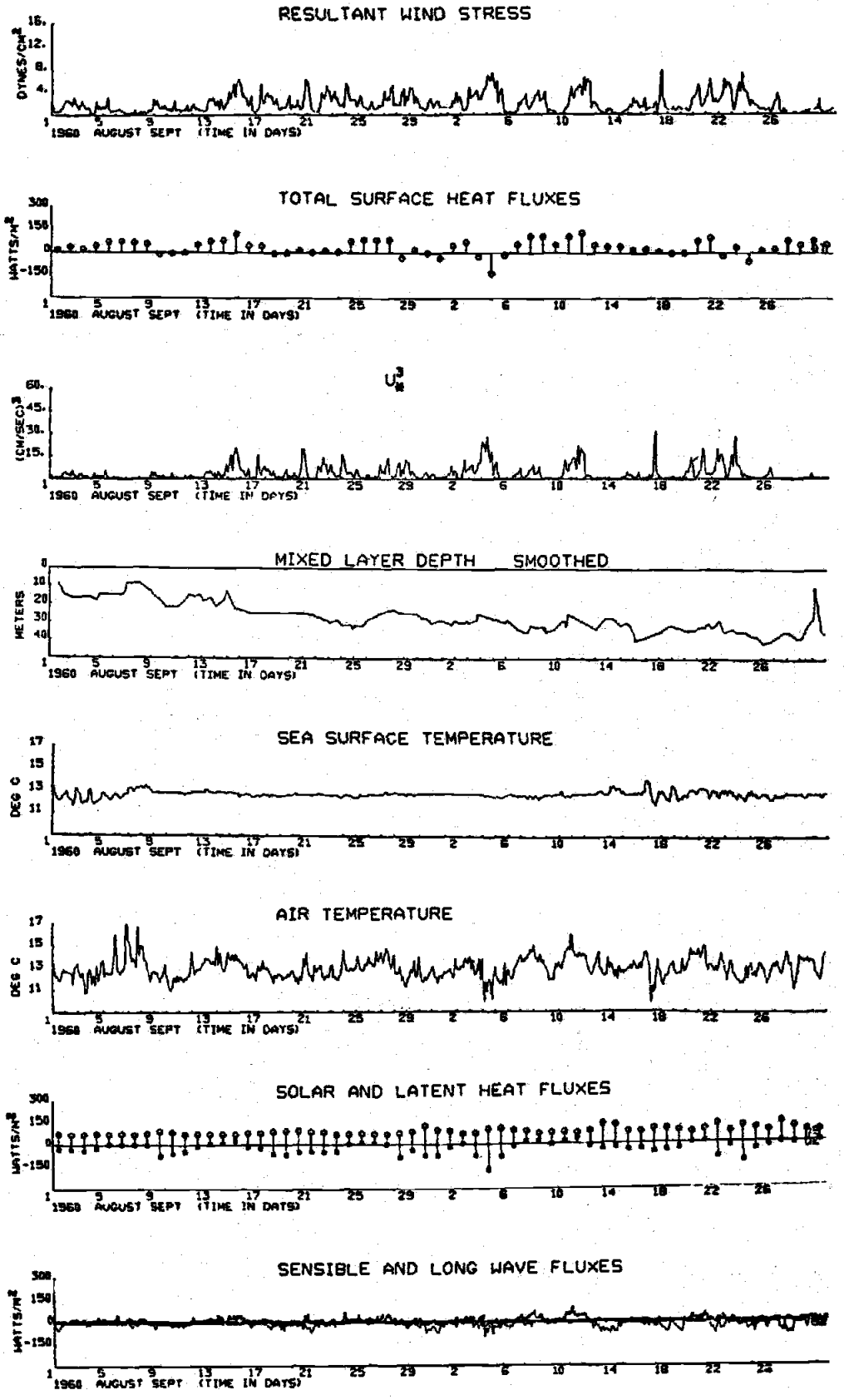
RESULTANT WIND STRESS
DYNES/CM²
TOTAL SURFACE HEAT FLUXES
WATTS/M²
U_{10}^3
(CM/SEC)³
MIXED LAYER DEPTH SMOOTHED
METERS
SEA SURFACE TEMPERATURE
DEG C
AIR TEMPERATURE
DEG C
SOLAR AND LATENT HEAT FLUXES
WATTS/M²
SENSIBLE AND LONG WAVE FLUXES
WATTS/M²
1960 AUGUST SEPT (TIME IN DAYS)

Figure 4

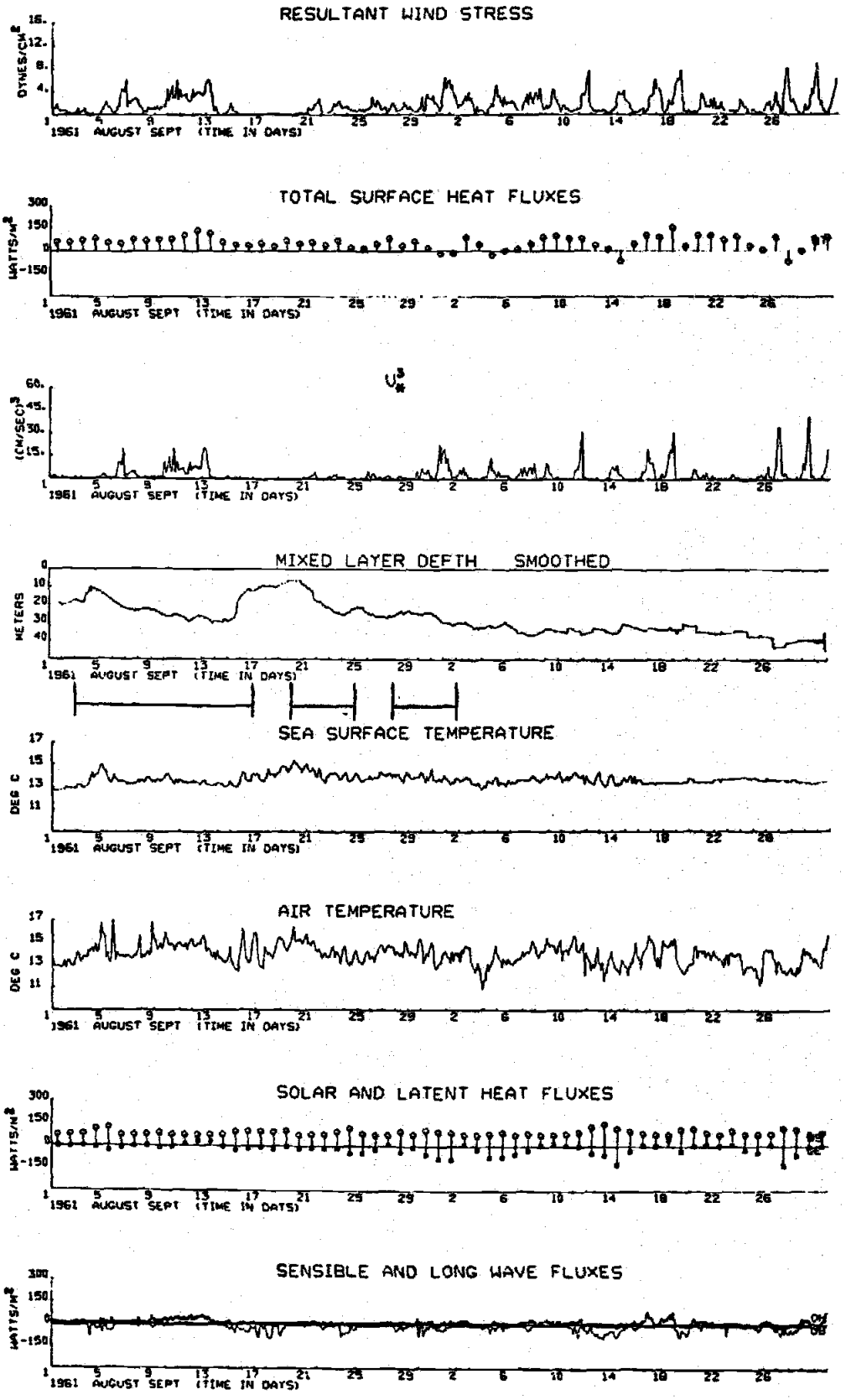
RESULTANT WIND STRESS
DYNES/CM²
TOTAL SURFACE HEAT FLUXES
WATTS/M²
(CM/SEC)³
MIXED LAYER DEPTH SMOOTHED
METERS
SEA SURFACE TEMPERATURE
DEG C
AIR TEMPERATURE
DEG C
SOLAR AND LATENT HEAT FLUXES
WATTS/M²
SENSIBLE AND LONG WAVE FLUXES
WATTS/M²
1961 AUGUST SEPT (TIME IN DAYS)

Figure 5

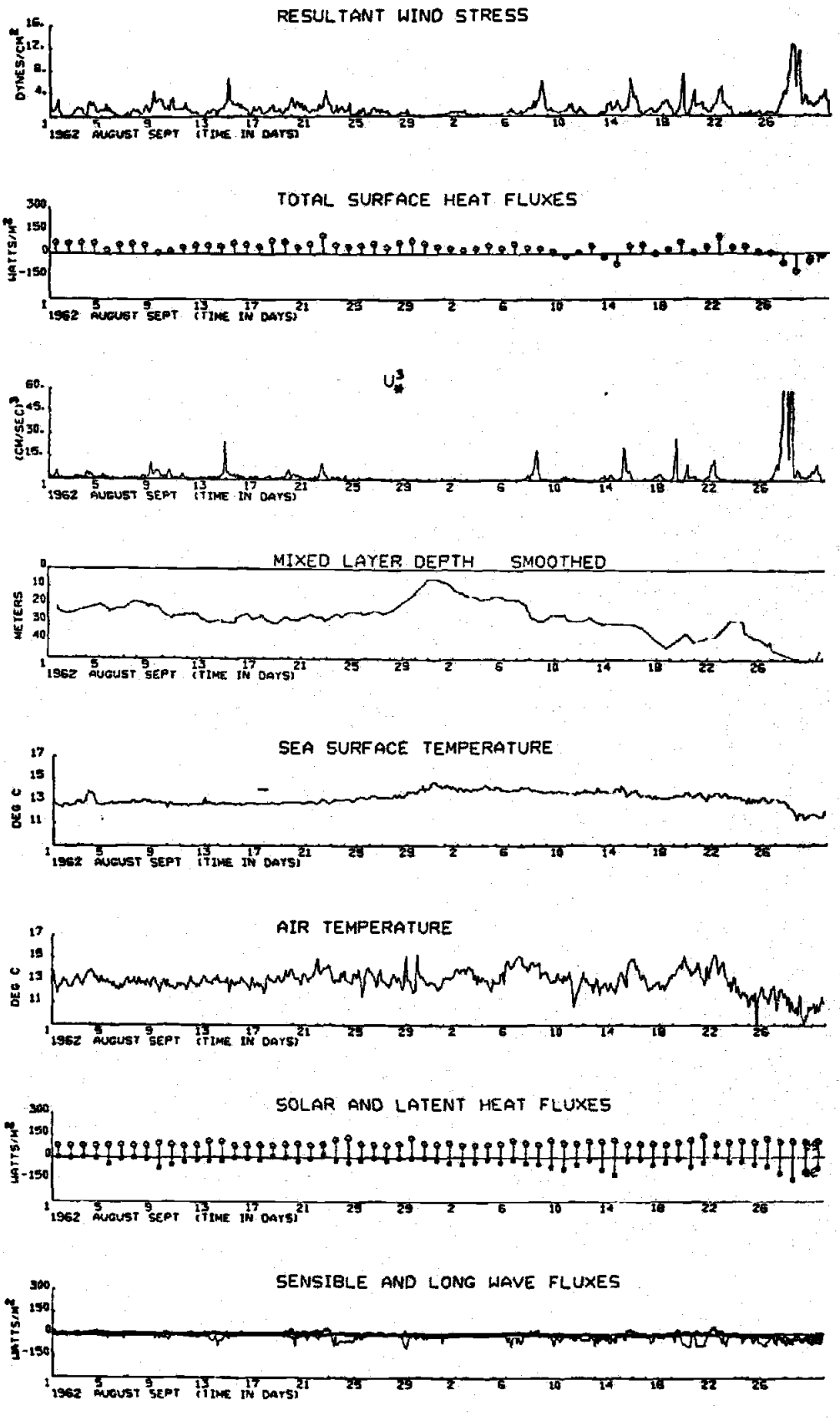
RESULTANT WIND STRESS
DYNES/CM²
16.
12.
8.
4.
1962 AUGUST SEPT (TIME IN DAYS)
TOTAL SURFACE HEAT FLUXES
WATTS/M²
300
150
0
-150
1962 AUGUST SEPT (TIME IN DAYS)
U*³
(CM/SEC)³
60.
45.
30.
15.
1962 AUGUST SEPT (TIME IN DAYS)
MIXED LAYER DEPTH SMOOTHED
METERS
0
10
20
30
40
1962 AUGUST SEPT (TIME IN DAYS)
SEA SURFACE TEMPERATURE
DEG C
17
15
13
11
1962 AUGUST SEPT (TIME IN DAYS)
AIR TEMPERATURE
DEG C
17
15
13
11
1962 AUGUST SEPT (TIME IN DAYS)
SOLAR AND LATENT HEAT FLUXES
WATTS/M²
300
150
0
-150
1962 AUGUST SEPT (TIME IN DAYS)
SENSIBLE AND LONG WAVE FLUXES
WATTS/M²
300
150
0
-150
1962 AUGUST SEPT (TIME IN DAYS)

Figure 6

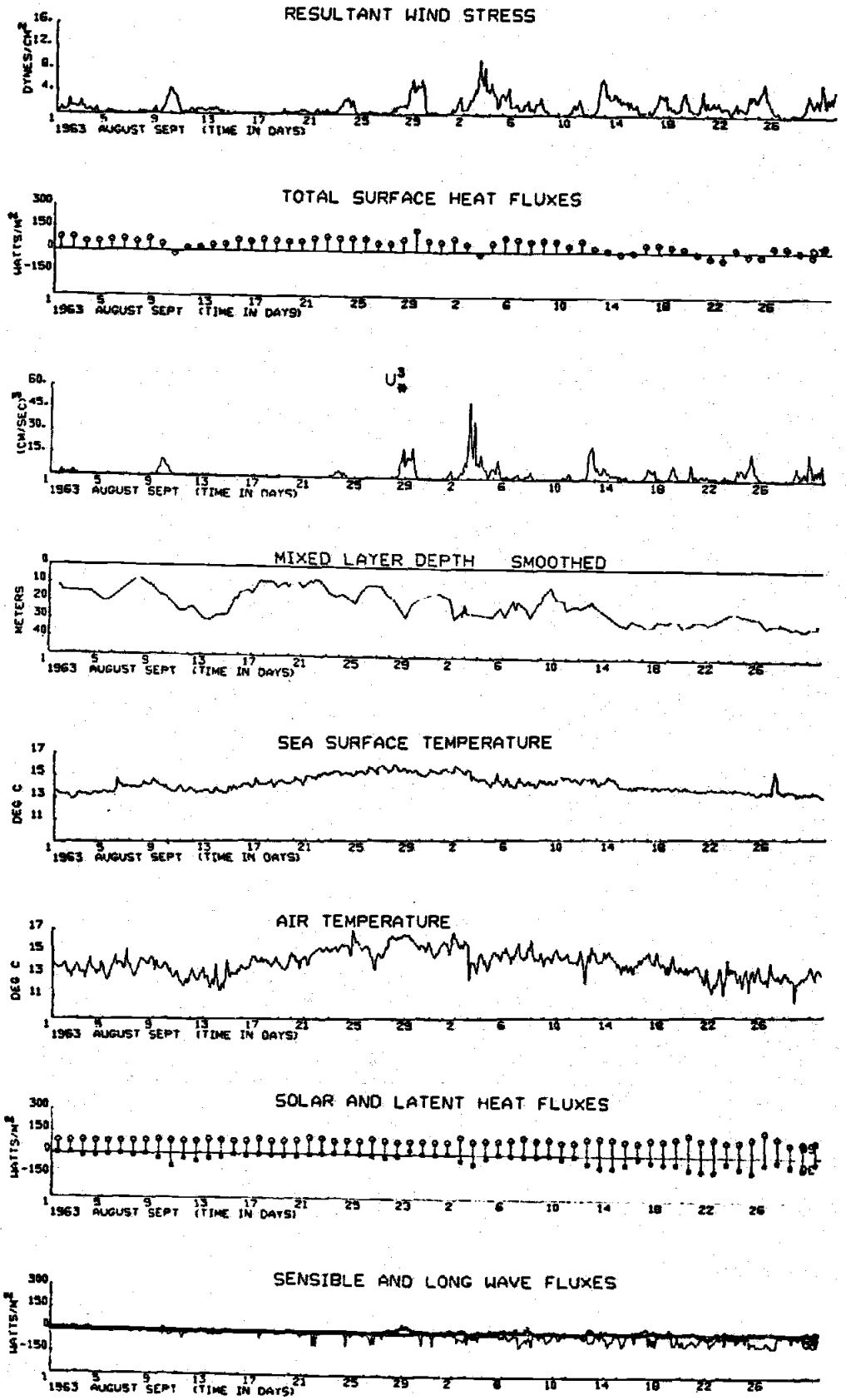
RESULTANT WIND STRESS
DYNES/CM²
16.
12.
8.
4.
1963 AUGUST SEPT (TIME IN DAYS)
TOTAL SURFACE HEAT FLUXES
WATTS/M²
300
150
0
-150
1963 AUGUST SEPT (TIME IN DAYS)
U*³
(CM/SEC)³
60.
45.
30.
15.
1963 AUGUST SEPT (TIME IN DAYS)
MIXED LAYER DEPTH SMOOTHED
METERS
10
20
30
40
1963 AUGUST SEPT (TIME IN DAYS)
SEA SURFACE TEMPERATURE
DEG C
17
15
13
11
1963 AUGUST SEPT (TIME IN DAYS)
AIR TEMPERATURE
DEG C
17
15
13
11
1963 AUGUST SEPT (TIME IN DAYS)
SOLAR AND LATENT HEAT FLUXES
WATTS/M²
300
150
0
-150
1963 AUGUST SEPT (TIME IN DAYS)
SENSIBLE AND LONG WAVE FLUXES
WATTS/M²
300
150
0
-150
1963 AUGUST SEPT (TIME IN DAYS)

Figure 7

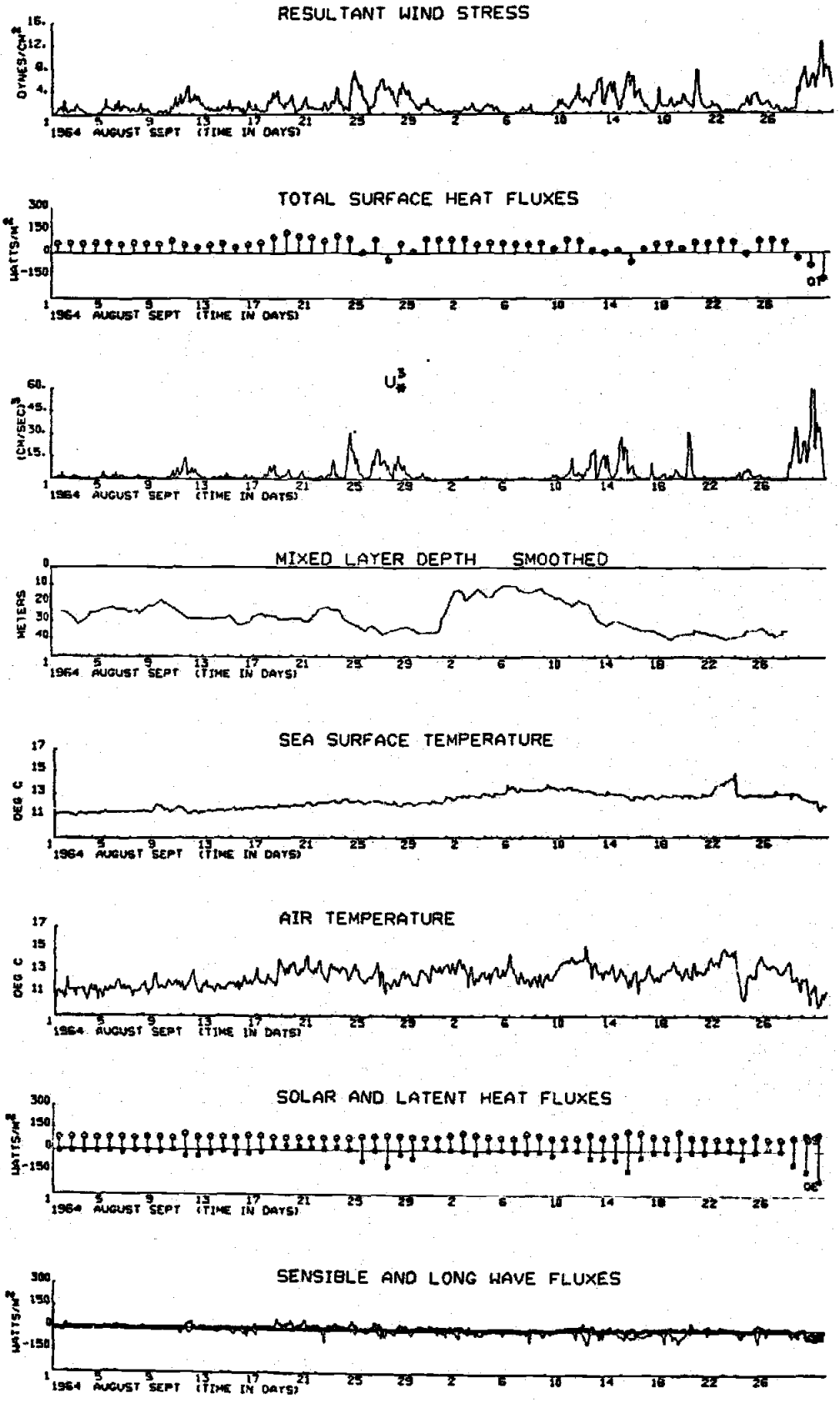
RESULTANT WIND STRESS
DYNES/CM²
16.
12.
8.
4.
TOTAL SURFACE HEAT FLUXES
WATTS/M²
300
150
0
-150
U*³
(CM/SEC)³
60.
45.
30.
15.
MIXED LAYER DEPTH SMOOTHED
METERS
0
10
20
30
40
SEA SURFACE TEMPERATURE
DEG C
17
15
13
11
AIR TEMPERATURE
SOLAR AND LATENT HEAT FLUXES
SENSIBLE AND LONG WAVE FLUXES
1964 AUGUST SEPT (TIME IN DAYS)

Figure 8

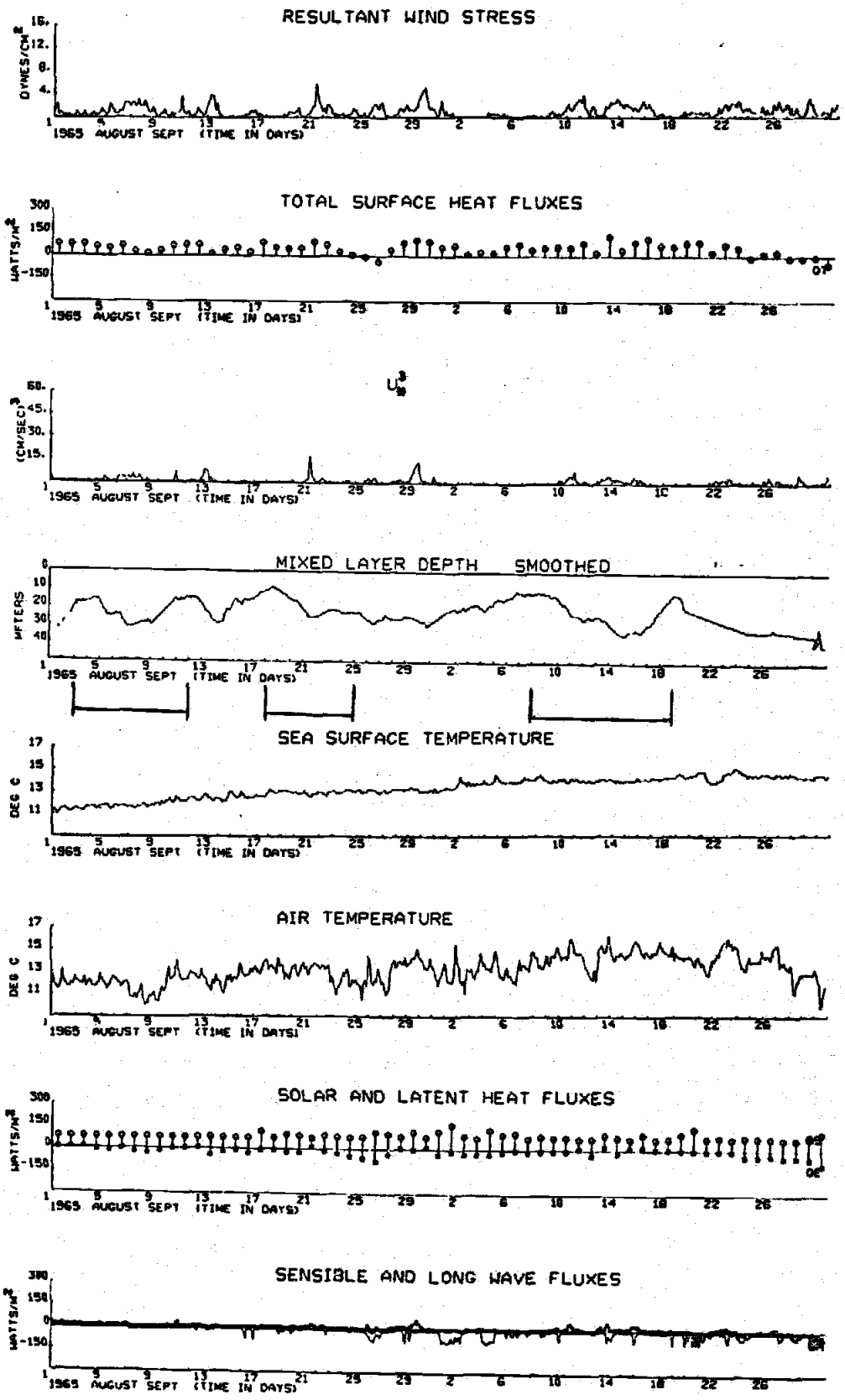
RESULTANT WIND STRESS
DYNES/CM²
1965 AUGUST SEPT (TIME IN DAYS)
TOTAL SURFACE HEAT FLUXES
WATTS/M²
MIXED LAYER DEPTH SMOOTHED
METERS
SEA SURFACE TEMPERATURE
DEG C
AIR TEMPERATURE
SOLAR AND LATENT HEAT FLUXES
SENSIBLE AND LONG WAVE FLUXES

Figure 9

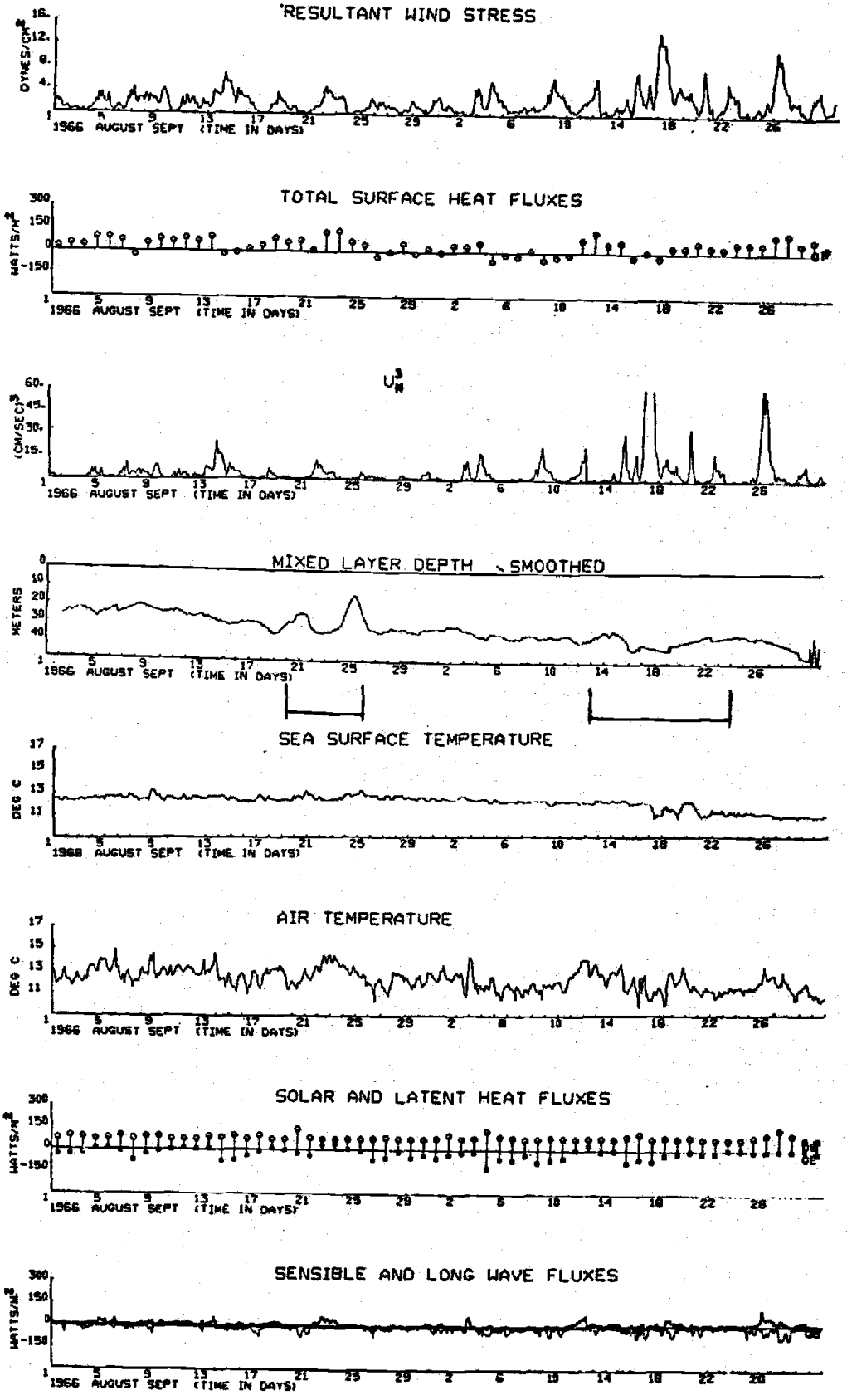
RESULTANT WIND STRESS
DYNES/CM²
16.
12.
8.
4.
1966 AUGUST SEPT (TIME IN DAYS)
TOTAL SURFACE HEAT FLUXES
WATTS/M²
300
150
0
-150
U_N^3
(CM/SEC)³
60.
45.
30.
15.
MIXED LAYER DEPTH - SMOOTHED
METERS
0
10
20
30
40
SEA SURFACE TEMPERATURE
DEG C
17
15
13
11
AIR TEMPERATURE
SOLAR AND LATENT HEAT FLUXES
SENSIBLE AND LONG WAVE FLUXES

Figure 10

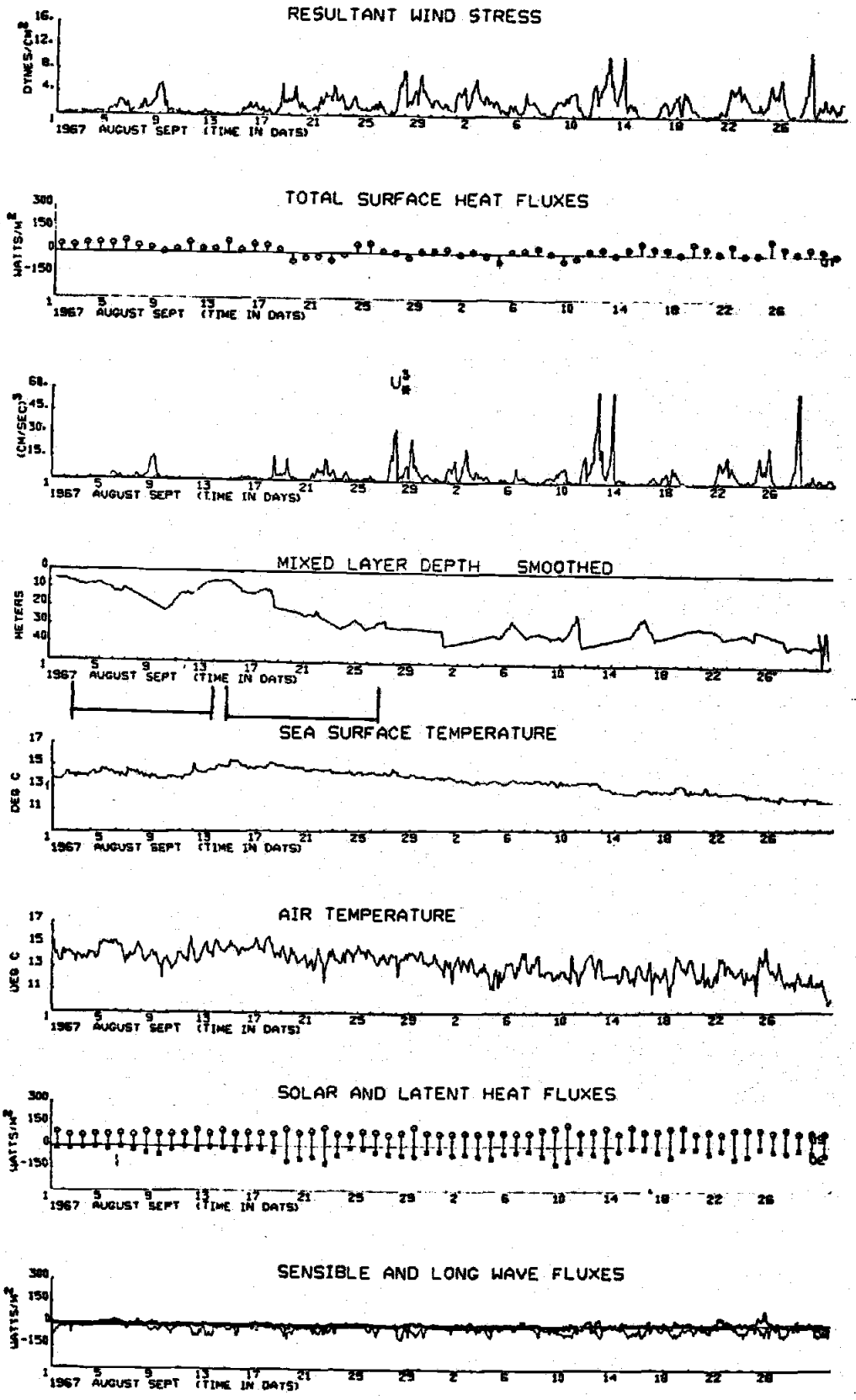
RESULTANT WIND STRESS
DYNES/CM²
16.
12.
8.
4.
1967 AUGUST SEPT (TIME IN DAYS)
TOTAL SURFACE HEAT FLUXES
WATTS/M²
300
150
0
-150
1967 AUGUST SEPT (TIME IN DAYS)
(CM/SEC)³
68.
45.
30.
15.
1967 AUGUST SEPT (TIME IN DAYS)
MIXED LAYER DEPTH SMOOTHED
METERS
0
10
20
30
40
1967 AUGUST SEPT (TIME IN DAYS)
SEA SURFACE TEMPERATURE
DEG C
17
15
13
11
1967 AUGUST SEPT (TIME IN DAYS)
AIR TEMPERATURE
DEG C
17
15
13
11
1967 AUGUST SEPT (TIME IN DAYS)
SOLAR AND LATENT HEAT FLUXES
WATTS/M²
300
150
0
-150
1967 AUGUST SEPT (TIME IN DAYS)
SENSIBLE AND LONG WAVE FLUXES
WATTS/M²
300
150
0
-150
1967 AUGUST SEPT (TIME IN DAYS)

Figure 11

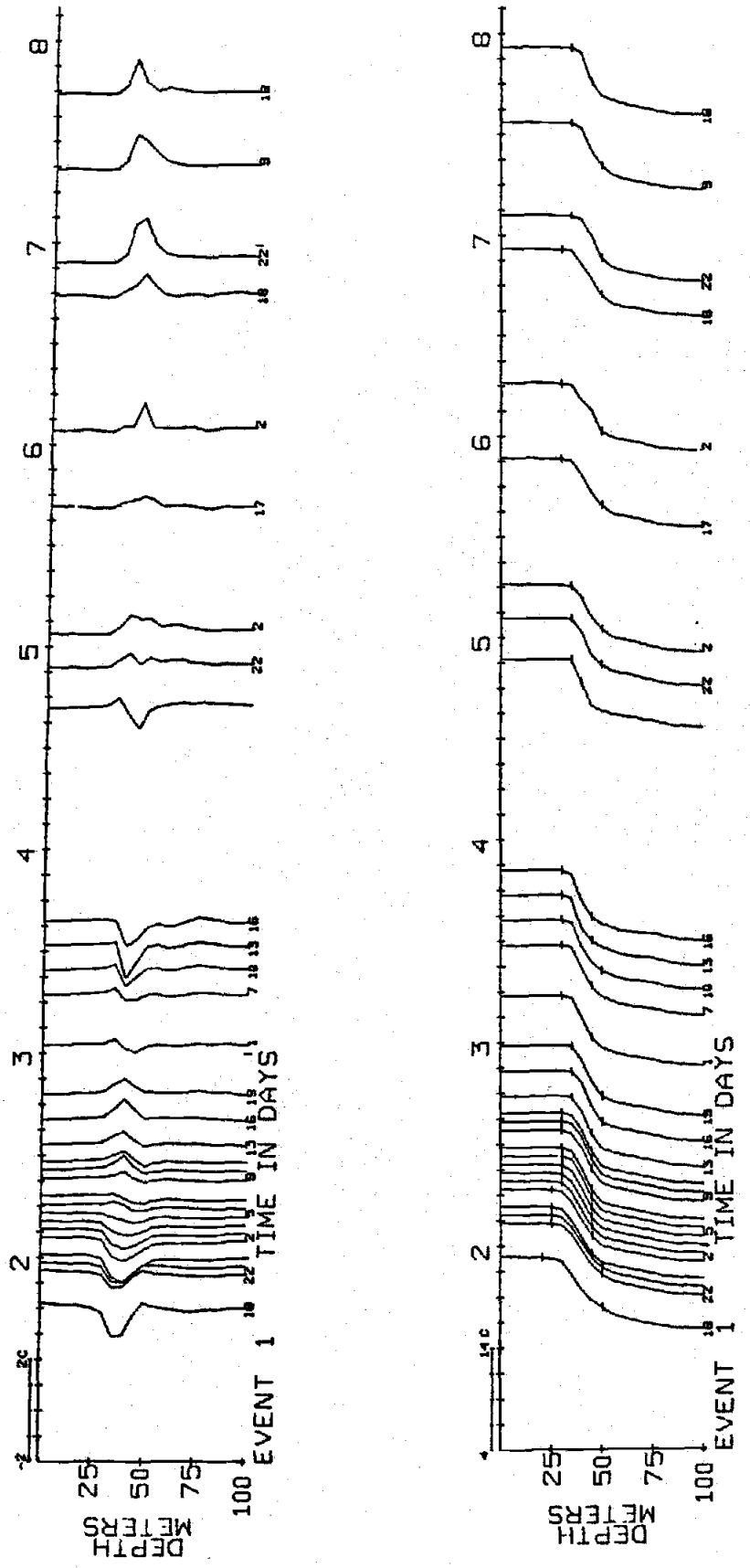

Figure 12

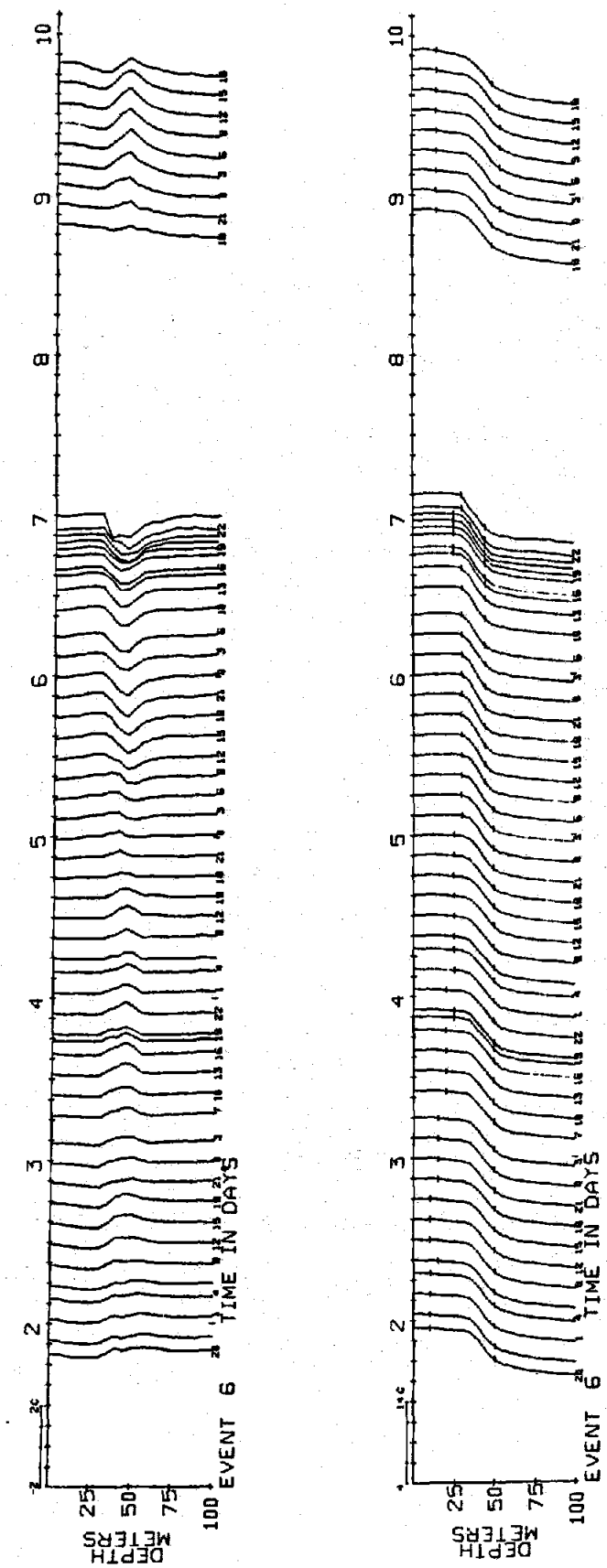
EVENT 6
TIME IN DAYS
DEPTH METERS
EVENT 6
TIME IN DAYS
DEPTH METERS

Figure 13

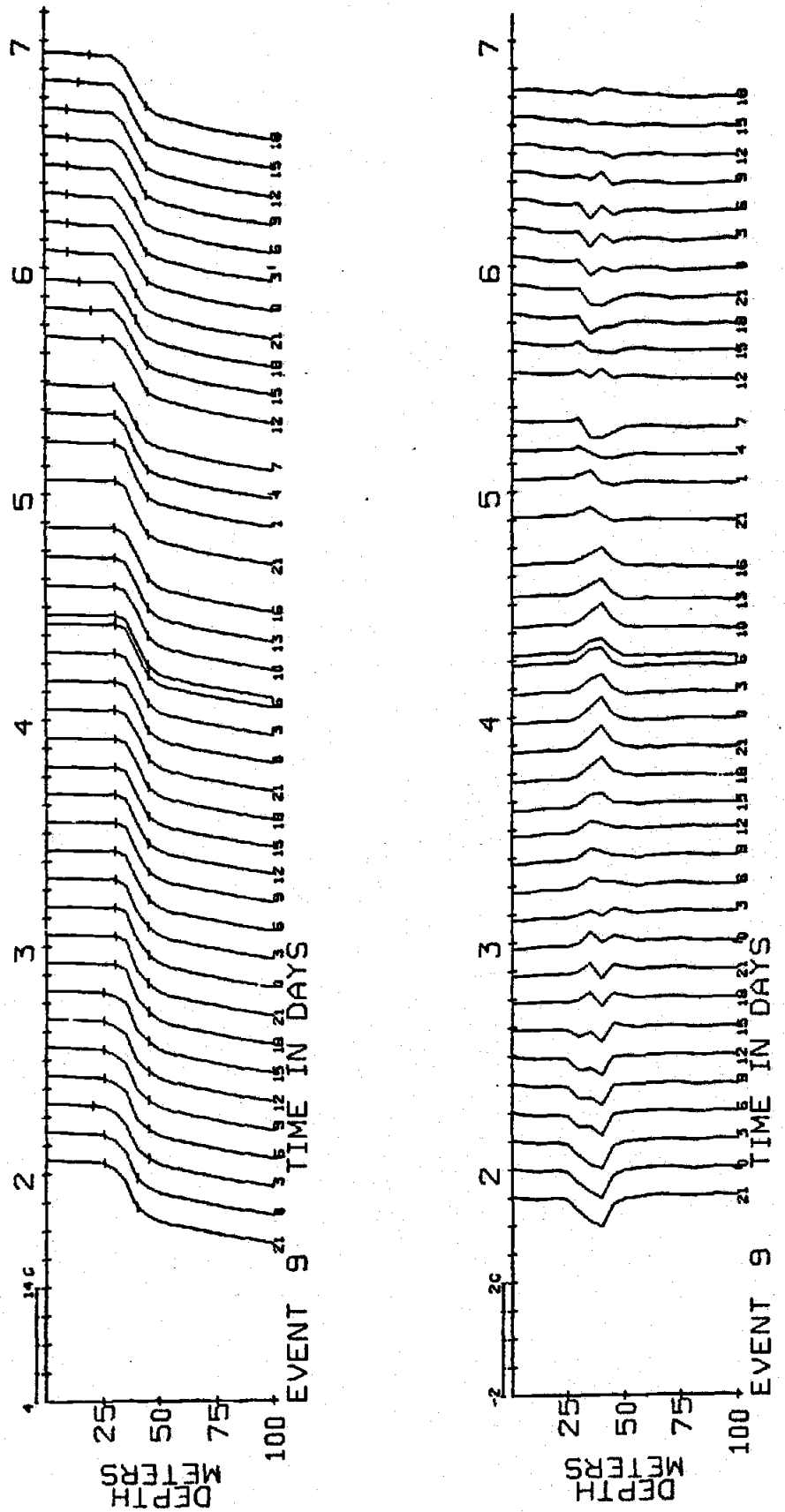
EVENT 9
TIME IN DAYS
DEPTH
METERS
EVENT 9
TIME IN DAYS
DEPTH
METERS

Figure 14

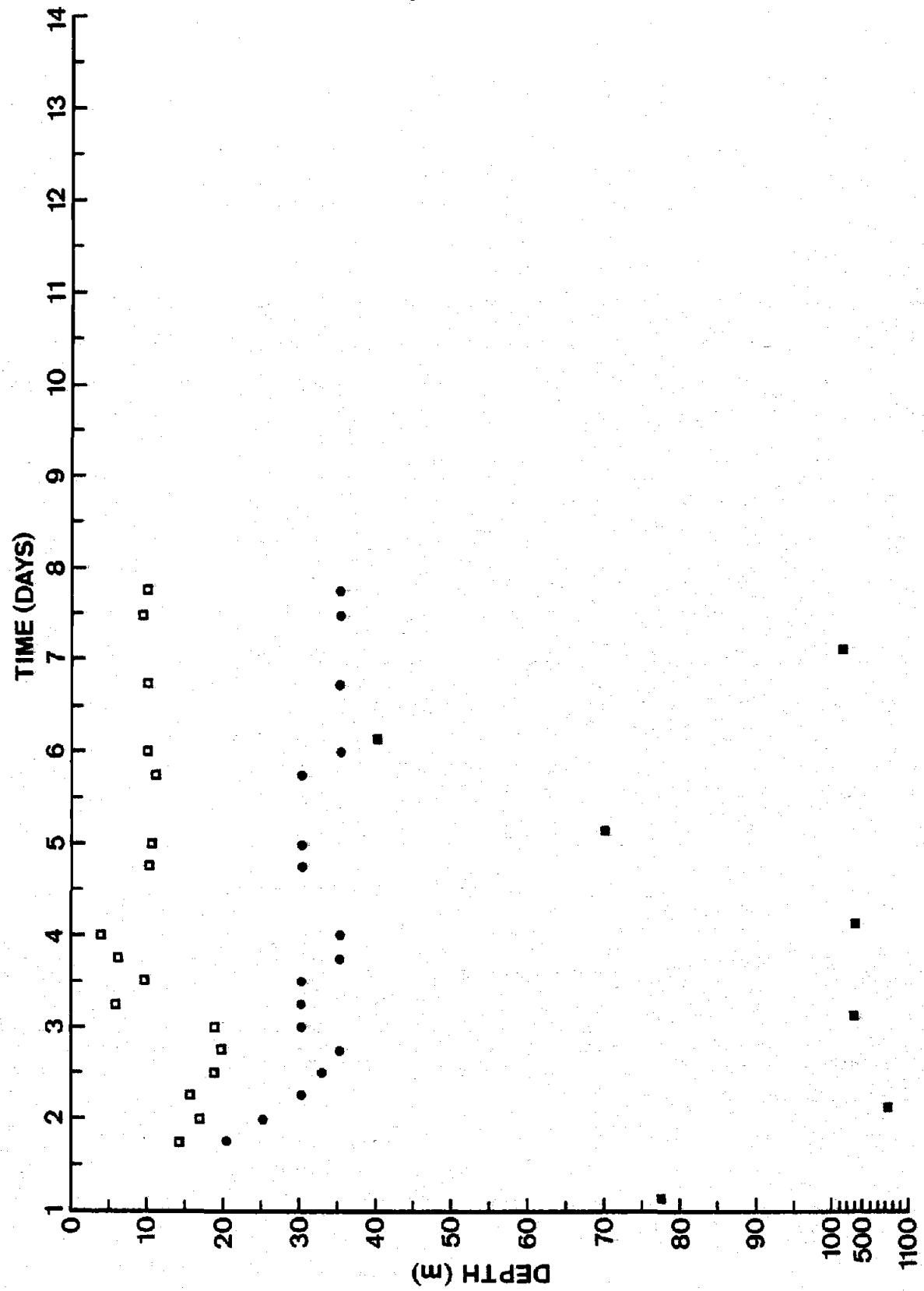
TIME (DAYS)
1
2
3
4
5
6
7
8
9
10
11
12
13
14
DEPTH (m)
0
10
20
30
40
50
60
70
80
90
100
500
1100

Figure 15

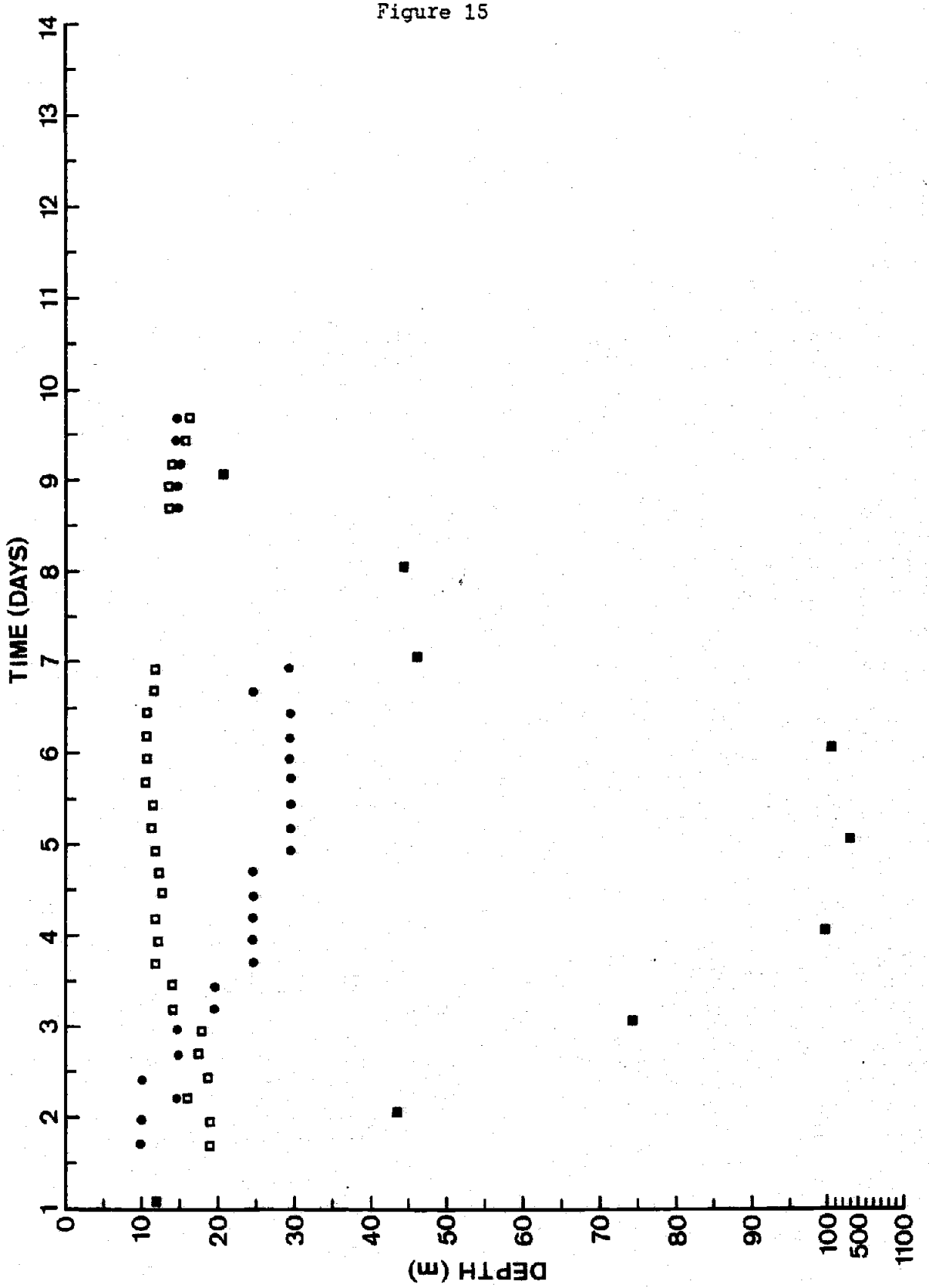
TIME (DAYS)
0
1
2
3
4
5
6
7
8
9
10
11
12
13
14
DEPTH (m)
0
10
20
30
40
50
60
70
80
90
100
500
1100

Figure 16

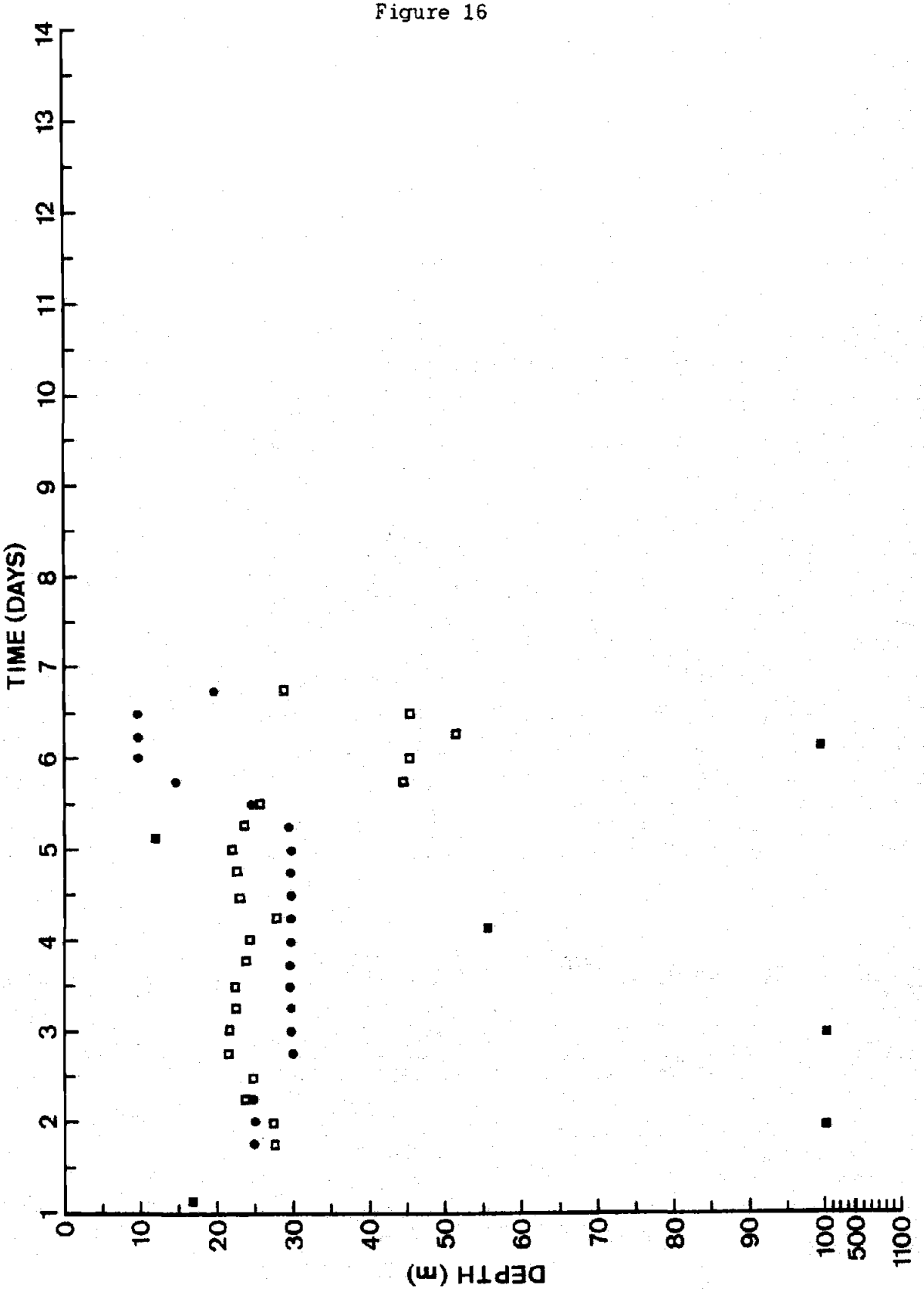
TIME (DAYS)
1
2
3
4
5
6
7
8
9
10
11
12
13
14
DEPTH (m)
0
10
20
30
40
50
60
70
80
90
100
500
1100

References

de Szoeke, R. A. and P. B. Rhines, 1976: Asymptotic regimes in mixed-layer deepening, J. Mar. Res., 34, 111-116.

Garwood, R. W., Jr., 1977: An oceanic mixed layer model capable of simulating cyclic states, J. Phys. Oceanogr., 3, 173-184.

Gill,A. E. and J. S. Turner, 1976: A comparison of seasonal thermocline models with observation, Deep-Sea Research, 23, 391-401.

Inbarne, J. V. and W. L. Godson, 1973: Atmospheric Thermodynamics, D. Reidel Publishing Company, Boston, Massachusetts, 222 pp.

Kim, Jeong-Woo, 1976: A generalized bulk model of the oceanic mixed layer, J. Phys. Oceanogr., 6, 686-695.

List, R. J., 1971: Smithsonian Meteorological Tables, Sixth edition, Smithsonian Institution, Washington, D.C., 527 pp.

Niiler, P. P., 1975: Deepening of the wind mixed layer, J. Mar. Res., 33, 405-422.

Niiler, P. P. and E. B. Kraus, 1977: One dimensional models of the upper ocean in Modeling and Prediction of the Upper Layers of the Ocean, ed. E. B. Kraus, Pergamon Press, New York, New York, 323 pp.

Paltridge, G. W. and C.M.R. Platt, 1976: Radiative Processes in Meteorology and Climatology, Elsevier Scientific Publishing Company, New York, New York, 314 pp.

Pollard, R. T., P. R. Rhines, and R.O.R.Y. Thompson, 1973: The deepening of the wind mixed layer, Geophys. Fluid Dyn., 3, 381-404.

Pond, S., D. B. Fissel, and C. A. Paulson, 1974: A note on the bulk aerodynamic coefficients for sensible heat and moisture fluxes, Boundary-Layer Meteorol., 6, 333-339.

Reed, R. K., 1976: On estimation of net long-wave radiation from the oceans, J. Geophys. Res., 81, (33), 5793-5794.

Reed, R. K., 1977: On estimating insolation over the ocean, J. Phys. Oceanogr., 7, 482-485.

Smith, S. D. and E. G. Banke, 1975: Variations of the sea surface drag coefficient with wind speed, Quart. J. Roy. Meteorol. Soc., 101, 665-673.

Tabata, Susumu, 1965: Variability of oceanographic conditions at Ocean Station "P" in the northeast Pacific Ocean, Trans. Roy. Soc. Can. Sect. III, Ser. 4, 3, 367-418.

Tully, J. P. and L. F. Giovando, 1963: Seasonal temperature structure in the eastern subarctic Pacific Ocean, in Roy. Soc. Can. Spec. Publ., 5, 10-36, M. J. Dunbar ed.